fire

MDPI

Article

Transferability of Empirical Models Derived from Satellite Imagery for Live Fuel Moisture Content Estimation and Fire Risk Prediction

Eva Marino [1,*], Lucía Yáñez [1], Mercedes Guijarro [2], Javier Madrigal [2], Francisco Senra [3], Sergio Rodríguez [3] and José Luis Tomé [1]

[1] Agresta S. Coop., Calle Duque de Fernán Núñez 2, 28012 Madrid, Spain; lyanez@agresta.org (L.Y.); jltome@agresta.org (J.L.T.)
[2] Instituto de Ciencias Forestales (ICIFOR-INIA), CSIC, Ctra. de La Coruña km 7,5, 28040 Madrid, Spain; guijarro@inia.csic.es (M.G.); incendio@inia.csic.es (J.M.)
[3] Agencia de Medio Ambiente y Agua, Junta de Andalucía, Calle Johan G. Gutenberg 1, 41092 Sevilla, Spain; francisco.senra.rivero@juntadeandalucia.es (F.S.); sergio.rodriguez@juntadeandalucia.es (S.R.)
* Correspondence: eva.marino.delamo@gmail.com

Abstract: Estimating live fuel moisture content (LFMC) is critical for assessing vegetation flammability and predicting potential fire behaviour, thus providing relevant information for wildfire prevention and management. Previous research has demonstrated that empirical modelling based on spectral data derived from remote sensing is useful for retrieving LFMC. However, these types of models are often very site-specific and generally considered difficult to extrapolate. In the present study, we analysed the performance of empirical models based on Sentinel-2 spectral data for estimating LFMC in fire-prone shrubland dominated by *Cistus ladanifer*. We used LFMC data collected in the field between June 2021 and September 2022 in 27 plots in the region of Andalusia (southern Spain). The specific objectives of the study included (i) to test previous existing models fitted for the same shrubland species in a different study area in the region of Madrid (central Spain); (ii) to calibrate empirical models with the field data from the region of Andalusia, comparing the model performance with that of existing models; and (iii) to test the capacity of the best empirical models to predict decreases in LFMC to critical threshold values in historical wildfire events. The results showed that the empirical models derived from Sentinel-2 data provided accurate LFMC monitoring, with a mean absolute error (MAE) of 15% in the estimation of LFMC variability throughout the year and with the MAE decreasing to 10% for the critical lower LFMC values (<100%). They also showed that previous models could be easily recalibrated for extrapolation to different geographical areas, yielding similar errors to the specific empirical models fitted in the study area in an independent validation. Finally, the results showed that decreases in LFMC in historical wildfire events were accurately predicted by the empirical models, with LFMC <80% in this fire-prone shrubland species.

Keywords: Sentinel-2; live fuel moisture content; wildfire; shrubland; *Cistus ladanifer*

check for updates

Citation: Marino, E.; Yáñez, L.; Guijarro, M.; Madrigal, J.; Senra, F.; Rodríguez, S.; Tomé, J.L. Transferability of Empirical Models Derived from Satellite Imagery for Live Fuel Moisture Content Estimation and Fire Risk Prediction. *Fire* **2024**, *7*, 276. https://doi.org/10.3390/fire7080276

Academic Editor: Alistair M. S. Smith

Received: 10 June 2024
Revised: 31 July 2024
Accepted: 2 August 2024
Published: 6 August 2024

Correction Statement: This article has been republished with a minor change. The change does not affect the scientific content of the article and further details are available within the backmatter of the website version of this article.

Copyright: © 2024 by the authors. Licensee MDPI, Basel, Switzerland. This article is an open access article distributed under the terms and conditions of the Creative Commons Attribution (CC BY) license (https://creativecommons.org/licenses/by/4.0/).

1. Introduction

Wildfires are a major threat worldwide, causing severe economic and environmental damage. In the context of climate change, extreme wildfire events are increasing in many regions of the world, with important loss of lives, infrastructures, and ecosystem services [1]. The main environmental drivers modifying wildfire activity are related to changes in weather and vegetation. At the landscape scale, the potential occurrence of large fires is strongly dependent on the spatial connectivity of dry fuel areas [2]. In the Mediterranean region, the projected increase in drought conditions due to climate change may lead to significantly larger burned areas and more frequent extreme wildfire behaviour [3–5].

Vegetation flammability is strongly conditioned by fuel moisture content (FMC), defined as the ratio of the weight of water in a fuel to the dry weight of the fuel, where dry

weight is made up of live and dead plant parts [6]. Traditionally, operational fire danger rating systems have focused on weather data, commonly using meteorological indices to estimate dead fuel moisture content, which is mainly affected by atmospheric conditions [7]. Live fuel moisture is generally one order of magnitude higher than dead fuel moisture and is often neglected in flammability and fire behaviour research, as live fuel is assumed to be more difficult to burn [1]. However, live fuel moisture content (LFMC) significantly affects ignition and fire rate of spread, as a higher water content implies more energy required to initiate and sustain vegetation combustion [8–10]. Estimation of LFMC is therefore critical for assessing vegetation flammability and potential fire behaviour, providing important information for wildfire prevention and management. Nonetheless, early warning systems predicting extreme wildfire events require reliable and spatially explicit estimation of vegetation moisture content and objective criteria for interpretation of predicted moisture patterns in terms of potential for major landscape fire occurrence [2]. For this purpose, historical analysis of LFMC values related to fire occurrence may be useful for establishing critical fire danger thresholds [11,12].

Although weather has an important effect on vegetation moisture content, models based only on meteorological indices are unable to accurately predict LFMC because the patterns of variation are highly dependent on other factors, such as species-specific plant physiology and soil characteristics [13–16]. Temporal and spatial LFMC dynamics are therefore linked to a combination of site characteristics, vegetation type (related to the different ecophysiological plant traits), species phenology and weather conditions [17], with the latter two being increasingly variable due to climate change [18].

The use of remote sensing has long been explored for LFMC monitoring with different methods [19]. Models based on satellite data have the advantage of being able to cover vast areas at various spatial and temporal resolutions, with varying results depending on the modelling approach (empirical models vs. radiative transfer models—RTM), the sensor used (active vs. passive) and the vegetation type (grassland, shrubland and woodland). Research has traditionally focused on satellite products from high-temporal-resolution sensors. Nonetheless, coarse spatial resolution (e.g., MODIS) and studies on medium-spatial-resolution sensors (e.g., Sentinel) are still scarce [20].

Previous research has demonstrated that empirical modelling based on spectral data derived from satellite sensors is useful for retrieving LFMC [11,21–23], with better results being obtained with visible and infrared data derived from optical sensors than with data derived from passive or active microwave sensors [24,25]. However, empirical models are often site-specific and are generally considered difficult to extrapolate to different geographical areas [19]. Conversely, RTM is a more complex, physically based approach, involving spectra simulations derived from optical sensors to obtain LFMC estimations independent of site specificities [26–28], but is less accurate for operational applications than empirical modelling [21,29].

In the present study, we focused on the assessment of models for estimating LFMC for operational use in fire danger rating systems based on field and remote sensing data. We analysed the performance of empirical models derived from Sentinel-2 data for LFMC monitoring in fire-prone shrubland dominated by *Cistus ladanifer,* a representative shrub that is widely distributed in the Western Mediterranean region, including the Iberian Peninsula, Southern France and north of Morocco and Algeria [30]. This shrub species is commonly used as a wildfire risk indicator species by fire management services in Spain because of its extensive distribution (nearly 3 million hectares, including monospecific shrubland and understorey in forest stands [31]) and also because the moisture content varies widely throughout the year [16,21,25]. The specific objectives of this study were as follows: (i) to extrapolate previous empirical models for the region of Madrid (central Spain) and the same shrubland species to a different geographical area in the region of Andalusia (southern Spain) and thus assess the potential transferability of the models accounting for site variability (spatial validation); (ii) to calibrate new empirical models with field data collected in the study area (region of Andalusia, southern Spain), comparing

the performance with that of previous existing models for the same shrubland type; and (iii) to test the performance of the best empirical model for predicting changes in LFMC below critical threshold values prior to historical wildfire events in order to assess the potential model transferability accounting for interannual variability (temporal validation).

2. Materials and Methods

2.1. Study Area and LFMC from Field Data

This study was conducted in the Sierra Morena, a mountain range covering 400 km in the region of Andalusia, southern Spain. Two sets of plots were established for LFMC monitoring by INIA (National Institute for Agricultural Research, from the Spanish Scientific Research Counsil-CSIC) and INFOCA (Andalusia Regional Fire Management Service), respectively, in the provinces of Huelva, Cordoba and Sevilla (Figure 1). The climate in the study area is Mediterranean type, with mild winters and hot summers and a precipitation regime generally characterised by a summer drought period.

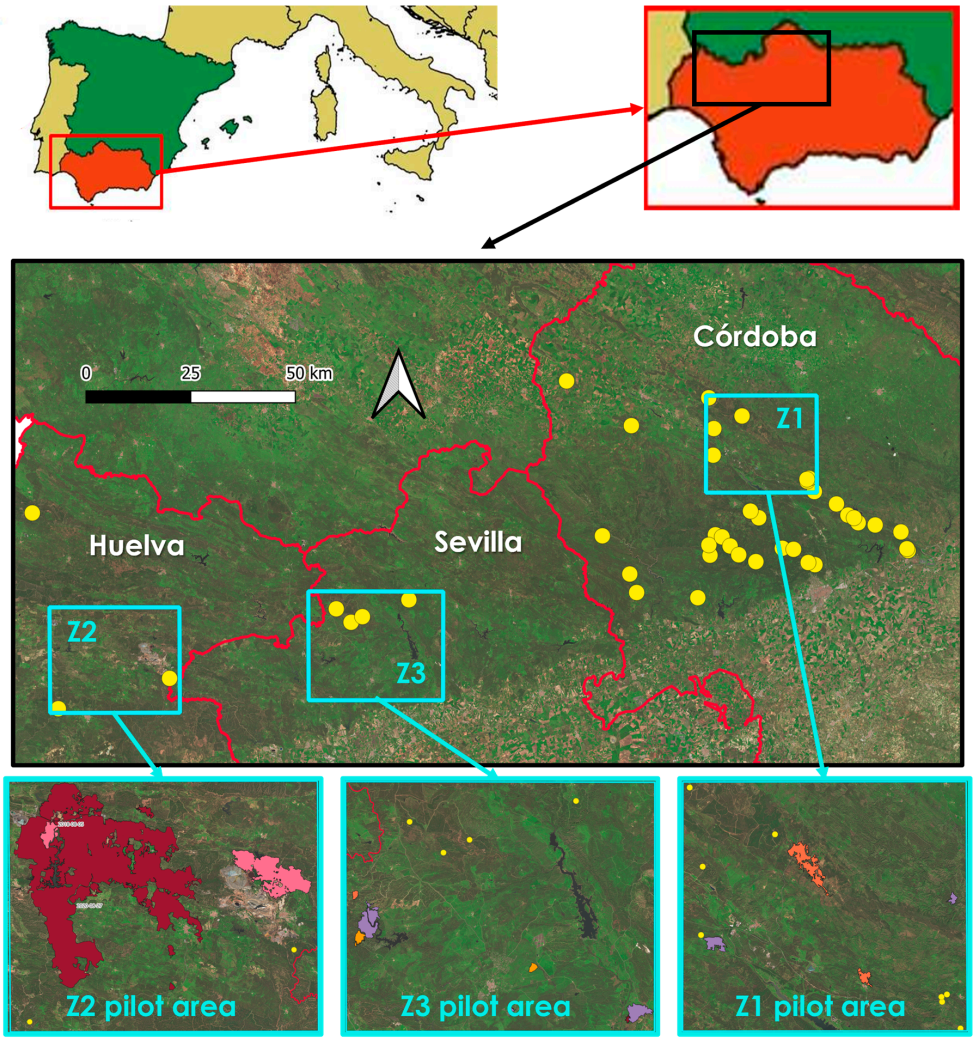

Figure 1. Study area (black rectangle) within the region of Andalusia (red) in Spain (green), with details on the location of the 27 sampling plots (INIA + INFOCA) and the historical wildfires (burnt areas for each year in different colours) in the pilot areas (Z1, Z2 and Z3).

The sampling plots were located in 27 different shrubland sites with *Cistus ladanifer* as a monospecific or dominant species (17 plots from INIA + 10 plots from INFOCA). Regarding vegetation functional type, this species is a summer semi-deciduous drought-avoider shrub with an accompanying water-spending strategy [27], and it is a typical pioneer species that

easily regenerates by seeds after disturbance and also coloniser in areas with recurrent wildfires [26]. Live vegetation samples were systematically collected throughout the year, at a higher frequency in the summer period (up to twice weekly). The methods regarding sampling and subsequent estimation of LFMC in the laboratory (the percentage of water content of vegetation on a dry-weight basis) are commonly used in similar studies and have been described in detail by Marino et al. [21]. Sampling dates included all seasons between June 2021 and September 2022, with two summer periods and a total of more than 400 registered LFMC values available as reference data.

In each province, a pilot area with several wildfires registered since 2018 was selected to assess the performance of the empirical models for LFMC estimation in historical wildfire events occurring next to the sampling plots in different years (Figure 1).

2.2. Remote Sensing Data

Field plot locations and sampling dates were used as reference data for selection of Sentinel-2 images in the study area, with a maximum time lag of two days when quality images on the exact sampling date were not available. The spectral information derived from the optical sensor Multi-Spectral Instrument (MSI) provided by the Sentinel-2 satellites (2A and 2B) was used, with a spectral resolution between the visible and the short-wave infrared (SWIR) registered in 13 bands at different spatial resolutions (10 m for visible and near-infrared (NIR), 20 m for red-edge and SWIR, and 60 m for atmospheric bands). A total of 782 images were available for the study period in the sampling plots, with up to 4 images in some locations for a certain date due to different "tiles" and overlapping of sensor paths.

Sentinel-2 Level-2A data were processed in the Google Earth engine (GEE) platform, providing bottom-of-atmosphere (BOA) reflectance corrected for geometric and radiometric effects. Shadowed pixels were masked out to prevent noise. Based on previous research using Sentinel-2 for LFMC estimation [21–23,25], spectral indices (SI) were selected (Table 1) and calculated at 20 m resolution. In some cases, SI were tested with two formulations, including band 8 and band 8A, respectively, as both bands measure similar wavelengths but have different bandwidths and central wavelengths. For each sampling date, the SI were calculated as the mean value of the pixels intersecting a circular area of a 10 m buffer radius centred in each sampling plot location.

Table 1. Spectral indices (name, abbreviation and Sentinel-2 bands) assessed for LFMC estimation.

Spectral Index	Abbreviation	S2 Bands
Normalized Difference Vegetation Index	NDVI	B8, B4
	NDVI 8A	B8A, B4
Normalized Difference Moisture Index	NDMI	B8, B11
	NDMI 8A	B8A, B11
Global Vegetation Moisture Index	GVMI	B8, B11
	GVMI 8A	B8A, B11
Green Normalized Difference Vegetation Index	GNDVI	B8, B3
Normalized Difference Water Index	NDWI	B8, B12
Normalized Difference Red-Edge Index	NDI45	B5, B4
Normalized Difference Glacier Index	NDGI	B3, B4
Enhanced Vegetation Index	EVI	B8, B4, B2
	EVI 8A	B8A, B4, B2
Soil Adjusted Vegetation Index	SAVI	B8, B4
	SAVI 8A	B8A, B4
Visible Atmospherically Resistant Index	VARI	B3, B4, B2

In addition, Sentinel-2 images from several dates prior to selected wildfires in each pilot area (Figure 1) were also processed to calculate the SI and subsequently to estimate the LFMC by applying the best empirical model obtained. The aim of this procedure was to assess the model performance for previous historical high flammability events in the region of Andalusia and the potential correlation between wildfire occurrence and critical LFMC threshold values.

2.3. Data Analysis

2.3.1. Database Generation

Field LFMC data and spectral values were matched and checked to generate a common database for statistical analysis. From the complete set of spectral information (782 images available; see previous section for details), cloud cover (%) and SI anomalies (absent values) were revised to select a unique spectral value matching each sampling date and location. The process yielded 445 registered field observations with the corresponding spectral information according to the different SI obtained for each date. This initial database was then checked for outliers, i.e., anomalies in terms of reference values (field or laboratory errors in LFMC retrieval) and spectral values (errors in SI calculations), resulting in a final reference dataset of 335 field-spectral matched values that were used as the basis for the modelling and validation analyses.

2.3.2. Statistical Modelling

A correlation matrix was used for preliminary assessment of the relationship between spectral indices and the observed LFMC derived from field monitoring. The statistical methods used for empirical modelling included simple (LR) and multivariate linear regression (MLR) and nonlinear regression (NLR) formulations. Before regression analysis, the normality of the distribution of observed LFMC values was checked using the Shapiro–Wilk test. Logarithmic transformation of LFMC values were also tested in MLR models.

For each type of formulation, the best combination of SI was selected according to the significance level of the model and each variable included ($p < 0.05$), the adjusted coefficient of determination (R^2_{adj}, to compare goodness of fit between models with a different number of input variables), and two statistics describing the level of error: mean absolute error (MAE) and root mean square error (RMSE). All statistical analyses were performed in R Software [32]. The variance inflation factor (VIF) was calculated for each input variable, and those models with variables yielding VIF > 5 were excluded to avoid potential collinearity among predictors.

New models for the region of Andalusia were fitted with a subset of two thirds of the samples available (n = 224), and the other samples were retained for independent validation (n = 111). Both subsets of data (calibration and validation) were randomly selected by including observations for each year of the study period and ensuring that the inter- and intra-annual variability were representative of the whole range of LFMC values observed.

2.3.3. Validation and Recalibration of Empirical Models

Models fitted for the region of Madrid for LFMC estimation in *Cistus ladanifer* with spectral data derived from Sentinel-2 were applied to the complete database available for the region of Andalusia (n = 335) to assess the potential extrapolation of the models to a different geographical area. Empirical models described by Marino et al. [21] were completed with additional MLR and NLR formulations, fitted for the same location in Madrid, thus allowing a potential transferability assessment including a wider range of model types. These models resulted from spectral data extracted in a single plot located in a monospecific *Cistus ladanifer* shrubland between 2016 and 2019 [21]. Observed and predicted LFMC values in the Andalusia dataset were compared and previous models for the region of Madrid were recalibrated with simple linear regression.

Independent validation of the new models fitted for the region of Andalusia with the calibration dataset (Section 2.3.1) was also performed. The correlation between estimated

and observed LFMC (R^2) was considered, together with error levels (MAE and RMSE), to evaluate and compare the performance of both sets of models: the empirical models previously fitted for the region of Madrid and transferred to the study area and the new empirical models fitted with the calibration data for the region of Andalusia.

2.3.4. LFMC Estimation in Historical Wildfires

Pilot areas (Figure 1) were used to assess the transferability potential of LFMC models in previous wildfire events accounting for interannual variability (temporal validation). Historical fire occurrence in the region of Andalusia was reviewed and wildfires of different sizes that burned in the pilot areas next to the field reference plots between 2018 and 2022 were selected for study. The performance of the best empirical model for predicting LFMC variability and decrease below critical threshold values was tested in the selected wildfire events, estimating LFMC from Sentinel-2 images acquired on previous dates. For each date, the LFMC considered was the mean value retrieved from the reference plots adjacent to each wildfire, used to analyse the evolution of vegetation moisture prior to ignition.

3. Results

3.1. LFMC Data from Field Monitoring

Field sampling data assessment confirmed the high variability of LFMC in *Cistus ladanifer* throughout the year, depending on species phenology and weather conditions, with values ranging from 45% to 205%. These values were similar to LFMC reported for this shrub species by Chuvieco et al. [11] and Marino et al. [21] in different Mediterranean areas of central Spain but with a wider range (both in term of minimum and maximum LFMC) than the values reported by Yebra et al. [26]. The wide range of variability in LFMC between plots within the study area for the same sampling date (up to 100%) is also noteworthy, especially during autumn, winter and spring, highlighting the high spatial heterogeneity in terms of moisture content for this shrubland species even in a similar geographical environment (Figure 2). This is particularly important in INIA plots, which were all located in a relatively limited area of the Sierra Morena in the province of Cordoba (45 km × 75 km).

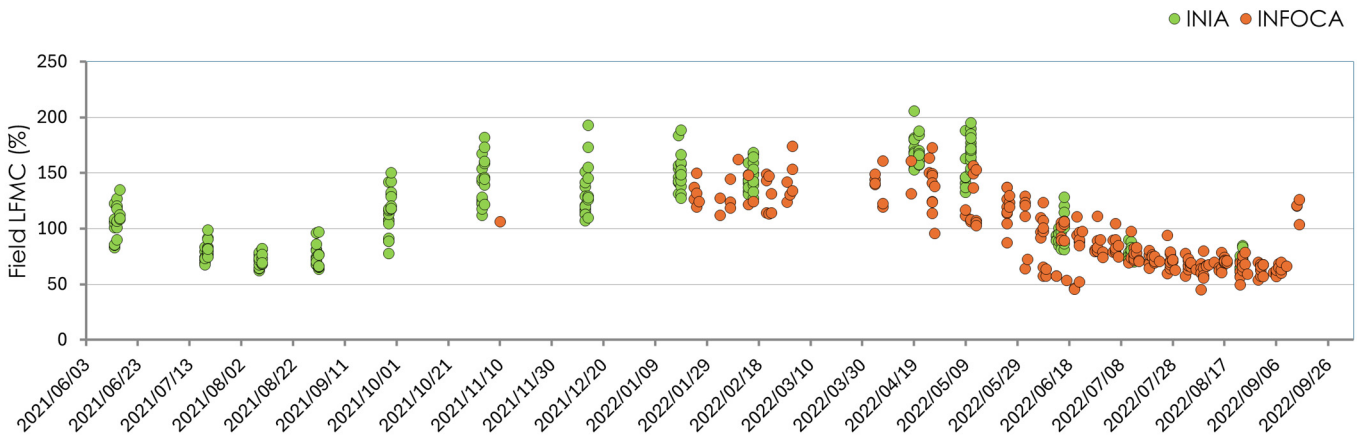

Figure 2. Observed LFMC values in INIA (green) and INFOCA (orange) field sampling plots during the study period (June 2021 to September 2022).

3.2. Correlation between LFMC and Spectral Indices

Results showed that all spectral indices had a Pearson correlation coefficient (r) with LFMC below 0.80 (Figure 3). The best indices were VARI (r = 0.797), EVI (r = 0.786), NDGI (r = 0.76), GVMI (r = 0.732) and NDMI (r = 0.73).

Some indices were strongly correlated, yielding r > 0.90 (e.g., VARI with NDGI, NDVI with GNDVI and NDI45, and GVMI with NDWI), and they therefore cannot be included together as predictor variables in multivariate empirical models to avoid collinearity.

	LFMC	EVI	EVI8A	GNDVI	GVMI	GVMI8A	NDGI	NDI45	NDMI	NDMI8A	NDVI	NDVI8A	NDWI	SAVI	SAVI8A	VARI
LFMC	1.00															
EVI	0.79	1.00														
EVI8A	0.73	0.98	1.00													
GNDVI	0.35	0.44	0.42	1.00												
GVMI	0.73	0.79	0.74	0.65	1.00											
GVMI8A	0.70	0.77	0.75	0.69	0.99	1.00										
NDGI	0.76	0.81	0.78	0.32	0.81	0.79	1.00									
NDI45	0.29	0.39	0.40	0.97	0.62	0.66	0.35	1.00								
NDMI	0.73	0.84	0.77	0.32	0.90	0.86	0.86	0.29	1.00							
NDMI8A	0.71	0.85	0.82	0.38	0.92	0.91	0.85	0.36	0.98	1.00						
NDVI	0.48	0.57	0.55	0.98	0.77	0.79	0.50	0.96	0.47	0.52	1.00					
NDVI8A	0.44	0.54	0.53	0.98	0.73	0.77	0.46	0.97	0.42	0.49	1.00	1.00				
NDWI	0.65	0.79	0.74	0.71	0.97	0.96	0.77	0.69	0.87	0.89	0.81	0.77	1.00			
SAVI	0.67	0.86	0.84	0.82	0.85	0.85	0.68	0.78	0.71	0.74	0.90	0.87	0.89	1.00		
SAVI8A	0.60	0.82	0.83	0.84	0.80	0.83	0.62	0.82	0.62	0.69	0.90	0.90	0.84	0.98	1.00	
VARI	0.80	0.85	0.81	0.38	0.84	0.82	0.99	0.40	0.86	0.86	0.55	0.52	0.80	0.73	0.68	1.00

Figure 3. Pearson correlation coefficients for spectral indices and LFMC in the calibration dataset (values highlighted in dark blue denote stronger correlations, r > 0.90).

3.3. Extrapolation of LFMC Models from a Different Geographical Area

Results of validation of previously fitted empirical models for LFMC estimation in the region of Madrid with Sentinel-2 are shown in Table 2. Results of the independent validation with the complete dataset available in the region of Andalusia (n = 335) were satisfactory for all formulations in terms of goodness of fit for observed and predicted LFMC values (R^2 > 0.60, Table 2). The best fit was found for the nonlinear model with square root formulation (NLR-sqr, R^2 = 0.65) but the prediction errors were higher (RMSE = 25%, MAE = 20%) than the values previously reported by Marino et al. [21] (RMSE = 20%, MAE = 15%). The logarithmic formulation (NLR-log) yielded similar fit (R^2) and error levels (RMSE and MAE). However, the range of predicted values resulted in an unrealistic minimum LFMC for this shrub species (19%).

Table 2. Validation of empirical models fitted for the region of Madrid with LFMC data monitored in field plots in Andalusia.

Model	Formulation	Predicted Values		Validation (n = 335)		
		Min	Max	R^2_{adj}	RMSE	MAE
LR *	LFMC = a + bVARI	50.5	183.2	0.651	26.54	22.50
MLR *	LFMC = a + b·VARI + c·SAVI	50.5	222.2	0.644	26.38	20.35
NLR-log *	LFMC = a + b·log(1+VARI) + c·log(SAVI)	19.6	205.9	0.654	24.80	19.35
NLR-exp	LFMC = a·exp(b·VARI)·exp(c·SAVI)	65.8	279.5	0.601	31.06	23.38
NLR-sqr	LFMC = a + b·$(VARI)^{0.5}$ + c·$(SAVI)^{0.5}$	40.2	213.5	0.652	25.45	19.77

* Models previously reported by Marino et al. [21].

Linear regression between observed and predicted values resulted in model recalibrations that better extrapolated to the field plots in Andalusia, reducing error levels (Table 3) and decreasing LFMC overestimation (Figure 4). The predicted LFMC varied from 15% as the minimum value in the LR model (exceeding realistic underestimation) to 215% as the maximum value in the NLR-exp model (Table 3). RMSE (22–24%) and MAE (17–18%) were reduced with recalibration but still higher than errors observed in the Madrid site (RMSE = 14–15%, MAE = 11–13%) where the original models were calibrated [21]. While retaining the good fit in all formulations tested (R^2 from 0.60 to 0.65), the best model was the MLR model that included VARI and SAVI, which showed more realistic minimum predicted values (LFMC = 50%) than the LR model using VARI as the only input variable and without LFMC overestimation (maximum of 189%). Regarding nonlinear formulations, the best model was NLR-sqr, with predicted LFMC in a similar range to field values (41%

and 185%). However, Figure 4 shows that the estimation errors for lower LFMC (<100%), which are associated with higher fire risk, were minimized in the NLR-exp formulation (RMSE = 16%, MAE = 12%) relative to the other models (RMSE > 18%, MAE > 14%; see Table A1 in Appendix A for details).

Table 3. Performance of the empirical models fitted in the Madrid region after recalibration with LFMC data monitored in Andalusia field plots.

Model	Formulation	Predicted Values		Validation (n = 335)		
		Min	Max	R^2_{adj}	RMSE	MAE
LR	LFMC = a + bVARI	15.2	194.4	0.651	22.01	17.65
MLR	LFMC = a + b·VARI + c·SAVI	50.3	189.4	0.644	22.21	17.18
NLR-log	LFMC = a + b·log(1+VARI) + c·log(SAVI)	23.6	182.0	0.654	21.91	17.07
NLR-exp	LFMC = a·exp(b·VARI)·exp(c·SAVI)	64.1	215.7	0.601	23.52	18.25
NLR-sqr	LFMC = a + b·$(VARI)^{0.5}$ + c·$(SAVI)^{0.5}$	41.0	184.9	0.652	21.98	17.03

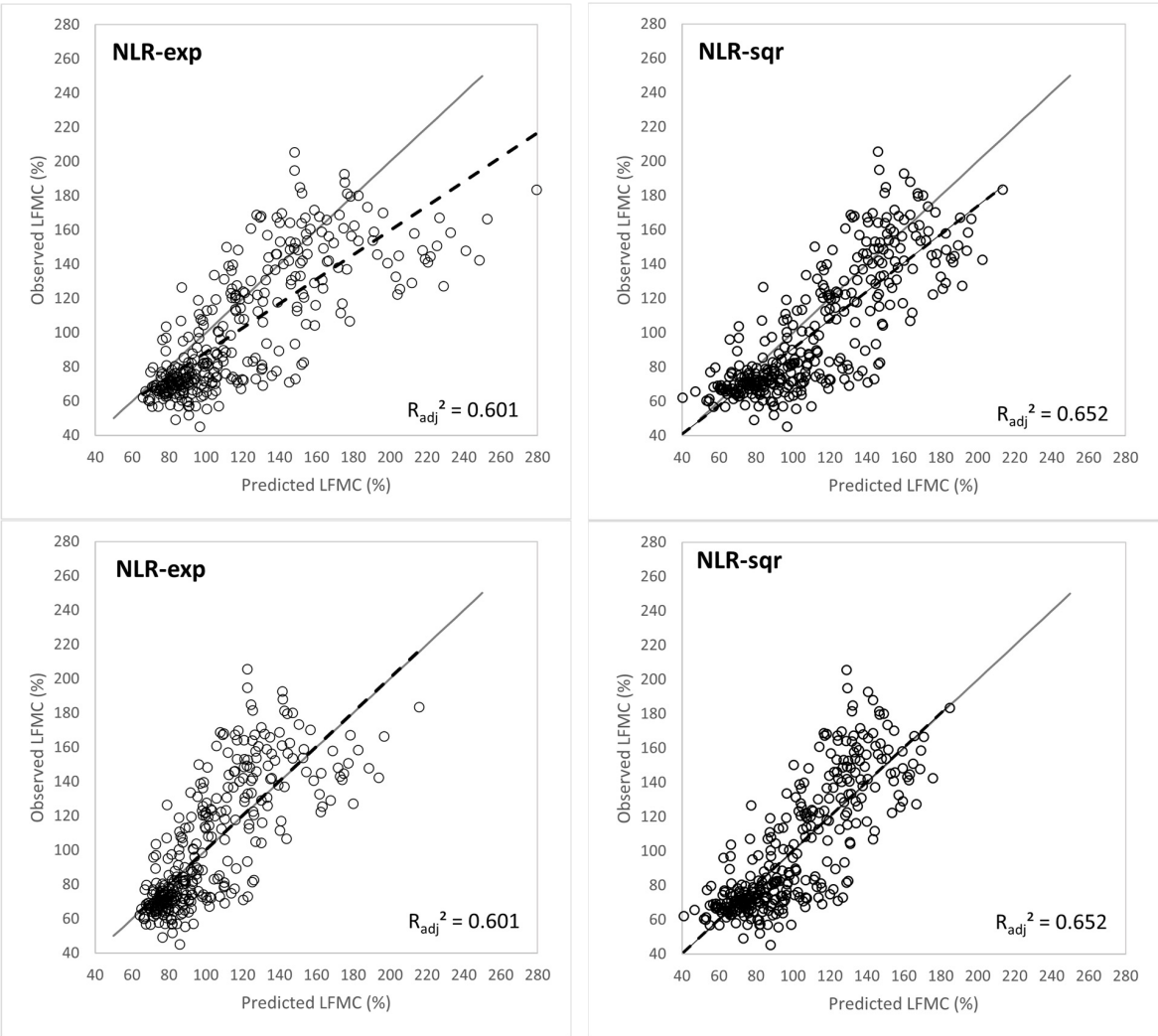

Figure 4. Extrapolation of the best empirical models previously fitted for the region of Madrid to the sampling plots in Andalusia, NLR-exp (**left**) and NLR-sqr (**right**), depicting validation results of original models (**upper**) and after recalibration (**lower**) with the linear regression (Y = a + bX) between observed and predicted values: NLR-exp (a = 17.33, b = 0.712); NLR-sqr (a = 7.659, b = 0.832). Y = recalibrated LFMC; X = predicted LFMC.

3.4. Calibration and Independent Validation of New LFMC Models Fitted in the Study Area

Results regarding models fitted in the region of Andalusia with the calibration subset of data (n = 224) are shown in Table 4 and Figure 5. For all formulations tested, the best combination for predicted LFMC was with VARI and EVI, which yielded a good fit (R^2 ranging from 0.70 to 0.72) and error level (RMSE = 20% and MAE ranging from 15% to 16%). In the case of EVI, the version of this SI obtained with band 8A was also tested, but R^2 slightly decreased in all models. Concerning the calibration dataset (field LFMC ranging from 49% to 205%), the best models were found for the exponential formulation (MLR-exp and NRL-exp) relative to the other models (i.e., lower R^2 or excessive underestimation in the LFMC predicted values). The nonlinear model (NLR-exp) yielded the best goodness of fit (R^2 = 0.72), with predicted values ranging from 56% to 210%, and a good error level (RMSE = 19.9% and MAE = 15.4%). However, the linear regression model obtained with log-transformation of the dependent variable (MLR-exp) also provided a good fit (R^2 = 0.71) while minimizing the prediction errors (MAE = 15.1%) in the calibration dataset.

Table 4. Empirical models fitted for the region of Andalusia with the LFMC calibration dataset. * MLR model fitted with logarithmic transformation of LFMC and spectral indices; ** MLR model fitted with logarithmic transformation of LFMC.

Model	Formulation	Predicted Values		Calibration (n = 224)		
		Min	Max	R^2_{adj}	RMSE	MAE
MLR	LFMC = a + b·VARI + c·EVI	52.0	181.6	0.708	19.71	15.57
MLR-pot *	LFMC = a·(1 + VARI)^b·EVI^c	51.5	198.0	0.699	19.76	15.26
MLR-exp **	LFMC = a·exp(b·VARI)·exp(c·EVI)	55.9	205.3	0.706	20.02	15.11
NLR-log	LFMC = a + b·log(1 + VARI) + c·log(EVI)	36.6	181.8	0.709	20.33	16.17
NLR-exp	LFMC = a·exp(b·VARI)·exp(c·EVI)	56.6	210.9	0.722	19.89	15.40
NLR-sqr	LFMC = a + b·(VARI)$^{0.5}$ + c·(EVI)$^{0.5}$	40.4	183.2	0.717	20.07	15.77

When assessing the performance of the models with the independent validation (n = 111) dataset (Table 5; Figure 6), the results confirmed that MLR-exp yielded the best accuracy and goodness of fit (R^2 = 0.69) relative to the other models, including NLR-exp, especially for the higher fire risk level (LFMC < 100%), with RMSE = 14.6% and MAE = 10.6%. The other formulations tested underestimated values relative to the observed LFMC in the validation dataset (ranging from 52% to 182%), except the log-transformed linear model (MLR-pot), which predicted a similar range of LFMC but was less accurate than MLR-exp for the higher fire risk level associated with LFMC < 100% (see Table A2 in Appendix A for details).

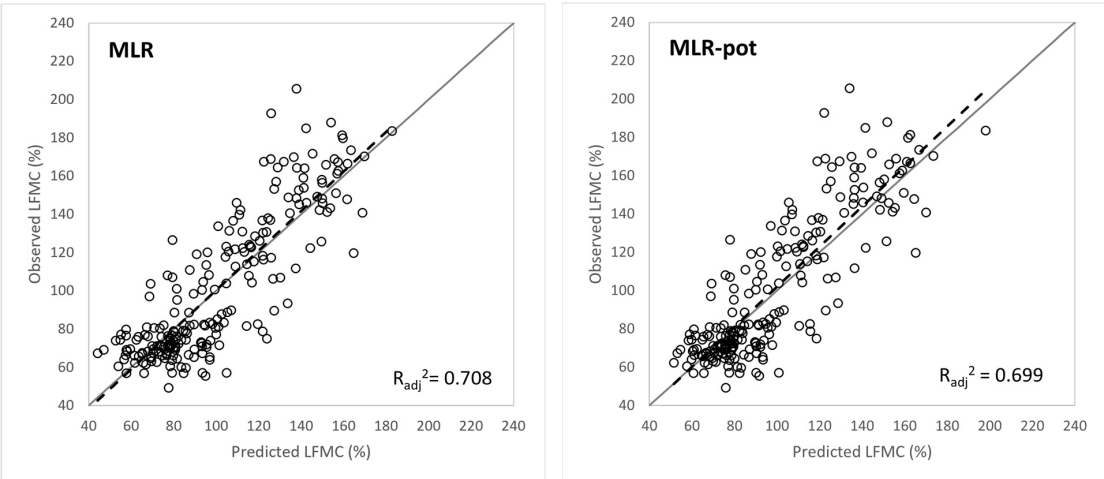

Figure 5. *Cont.*

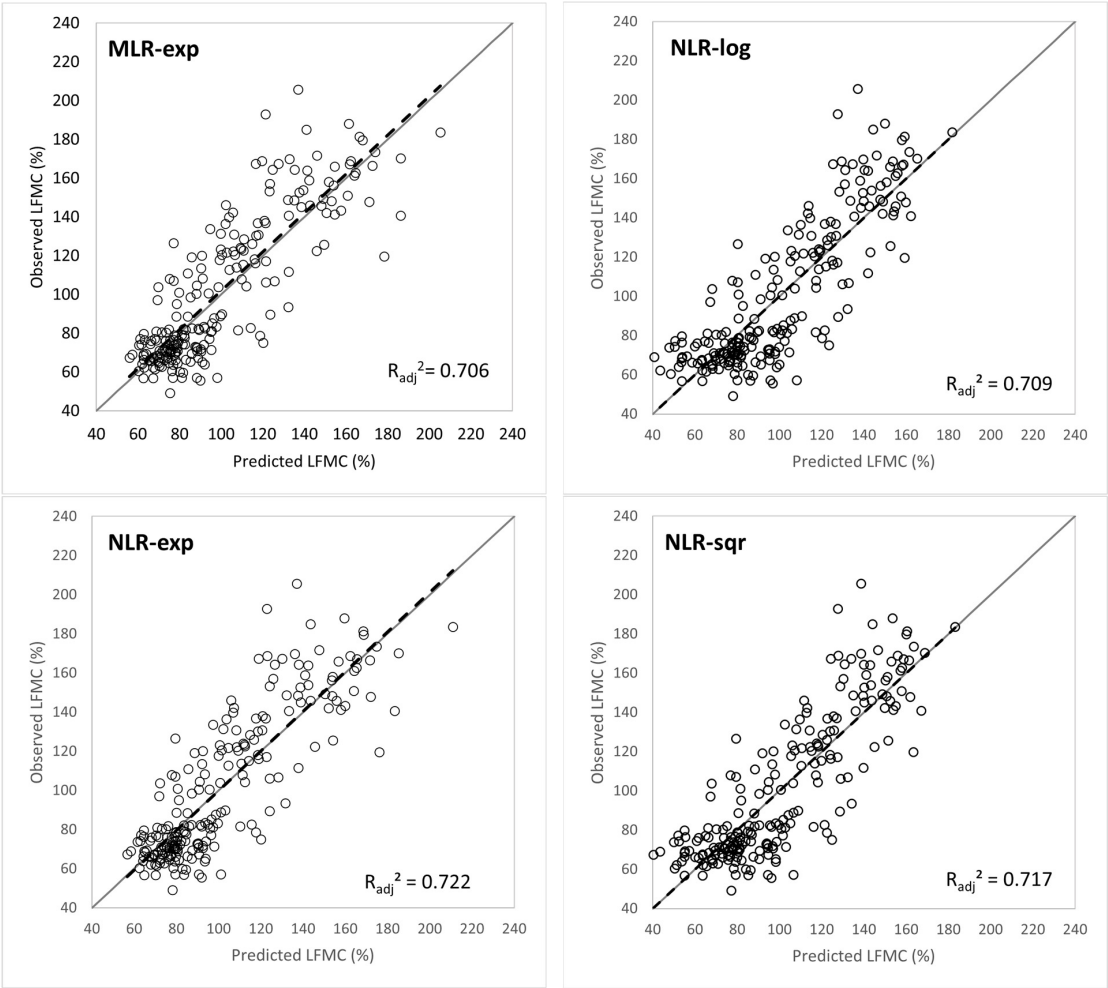

Figure 5. Observed vs. predicted LFMC values in the best models for each formulation tested with the calibration dataset (n = 224) for field plots in Andalusia.

Table 5. Performance of the empirical models fitted for the region of Andalusia with the LFMC independent validation dataset. * MLR model fitted with logarithmic transformation of LFMC and spectral indices; ** MLR model fitted with logarithmic transformation of LFMC.

Model	Formulation	Predicted Values		Validation (n = 111)		
		Min	Max	R^2_{adj}	RMSE	MAE
MLR	LFMC = a + b·VARI + c·EVI	49.7	173.4	0.686	19.92	15.73
MLR-pot *	LFMC = a·(1 + VARI)^b·EVI^c	56.0	184.5	0.693	19.75	15.40
MLR-exp **	LFMC = a·exp(b·VARI) ·exp(c·EVI)	58.4	186.9	0.694	19.78	15.26
NLR-log	LFMC = a + b·log(1 + VARI) + c·log(EVI)	44.0	174.4	0.677	20.25	16.10
NLR-exp	LFMC = a·exp(b·VARI) ·exp(c·EVI)	59.9	193.2	0.686	19.89	15.53
NLR-sqr	LFMC = a + b·(VARI)$^{0.5}$ + c·(EVI)$^{0.5}$	46.4	174.6	0.689	19.86	15.71

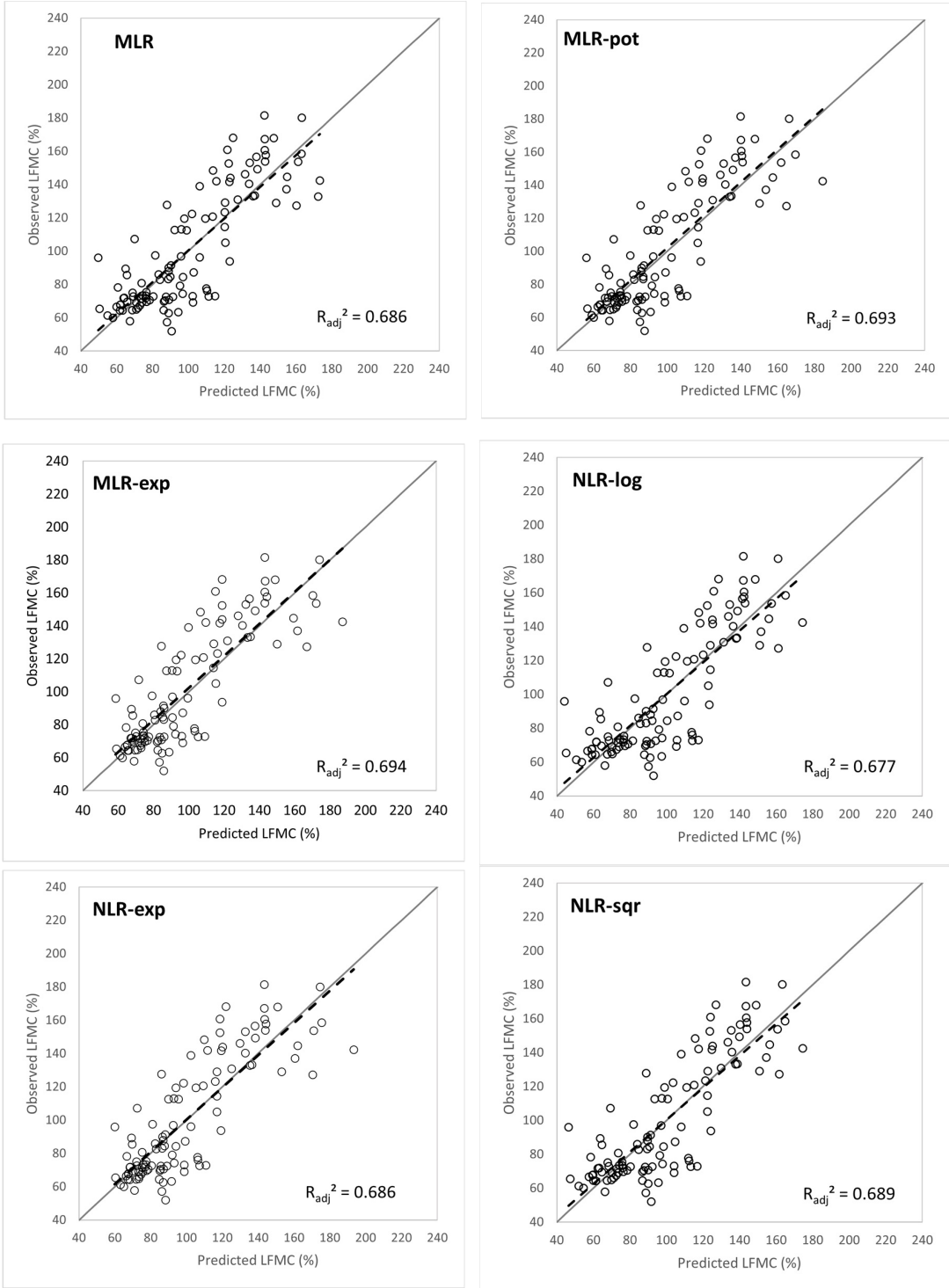

Figure 6. Observed vs. predicted LFMC values in the independent validation (n = 111) of the best models fitted for field plots in Andalusia.

3.5. Correlation between Historical Wildfire Occurrence and LFMC Estimated from Remote Sensing Data

In total, seven wildfires (Table 6) were selected in the pilot areas and used for testing the performance of the best empirical model (MLR-exp).

The trend analyses of the estimated LFMC in previous months showed that the empirical model successfully predicted the LFMC decrease in all wildfire events. Figure 7 depicts the changes in LFMC predicted by the model in the reference plots for the seven selected

wildfires according to the spectral information derived from Sentinel-2. An example of the LFMC raster maps, generated to assess the change in fire risk prior to the Almonaster wildfire, is provided in Appendix B (Figure A1). The Almonaster wildfire was the biggest event occurring in the region of Andalusia during the study period (2018–2022), resulting in a total area of 14,957 ha burned in 12 days.

Table 6. Historical wildfire selected in the pilot areas for LFMC model testing.

Pilot Area	Province	Wildfire Name	Ignition Date	Area Burned (ha)	Reference Plots
Z1	Córdoba	Alcaracejos	2021/08/16	379	3
		Espiel	2022/07/25	160	3
Z2	Huelva	Nerva	2018/08/02	1628	3
		Almonaster	2020/08/27	14,957	4
Z3	Sevilla	El Ronquillo	2021/07/28	43	3
		Guillena	2022/07/10	416	3
		Cantillana	2022/07/25	249	3

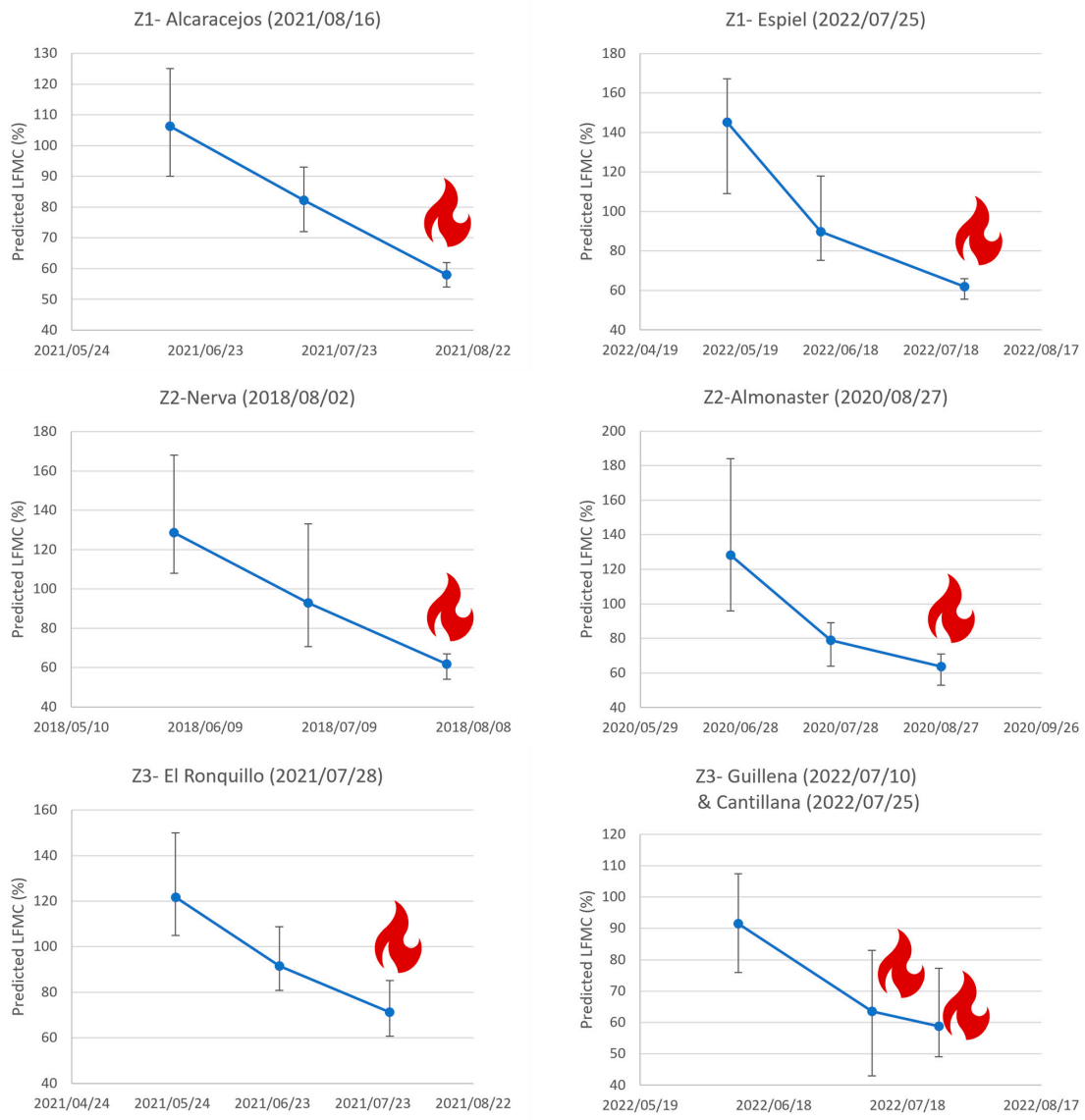

Figure 7. Performance of the best empirical model for LFMC estimation before the 7 selected historical wildfire events in the pilot areas (Z1, Z2 and Z3), depicting the mean value of reference plots available for each wildfire (blue) and the LFMC range for each date (vertical bars). Headings indicate the wildfire name, with the ignition date in brackets and depicted as red symbols.

4. Discussion

4.1. Spatial Transferability vs. Site-Specific LFMC Empirical Models

Extrapolation of empirical models previously fitted for the same shrubland species in a different geographical region (Madrid, central Spain) to the study area (Andalusia, southern Spain) showed that direct transferability of LFMC models based on remote sensing has limitations, even for the same monospecific vegetation. Some authors have assessed the spatial transferability of empirical models derived from satellite data, including LFMC estimation in shrubland and grassland, with moderate results [11]. In the present study, despite the good fit between observed and predicted LFMC in all formulations tested (R^2 from 0.60 to 0.65), RMSE and MAE were 5% higher (in absolute value) than the errors previously reported for independent validation of the empirical models in the Madrid region [21]. Nonetheless, our results confirmed the validity of transferring previous *Cistus ladanifer* models to different geographical areas with similar shrubland vegetation using a simple recalibration with field data. Once recalibrated, the existing models provided sufficiently reliable LFMC prediction for operational purposes, yielding good estimation errors (RMSE = 16%, MAE = 12%) under the higher fire risk scenarios (LFMC < 100%). Recalibration provided better results regarding the error level and, most importantly, decreased the undesired LFMC overestimation (predicted values higher than field values) that poses a major threat to wildfire risk assessment (Figure 4).

As expected, the model performance improved when site-specific empirical models based on field LFMC monitoring data available for the study region were fitted. The results showed a better fit between observed and predicted LFMC in the calibration (R^2 ranging from 0.70 to 0.72) as well as the independent validation (R^2 from 0.68 to 0.69). However, at lower LFMC values (<100%) the prediction errors were similar to those found in the extrapolation of previous models after recalibration (Tables A1 and A2). It is worth noting that previous models were fitted with data from a single plot in the region of Madrid [21], whereas the new models were derived from data from a set of 27 plots located in three different western provinces in the region of Andalusia. Moreover, the performance of the previous models may also be worse because lower LFMC values were less well represented in model calibration, as Sentinel-2 sensors were not fully operational for the whole study period (2016–2019), i.e., fewer images were available in Marino et al. [21]. Hence, extrapolation of the previous uncalibrated models was also biased towards overestimation, which is of greater concern for LFMC estimation at lower values (<100%). Our results confirm that empirical models perform better when calibrated carefully by including multiple sites and as wide a range of variability as possible in the field LFMC data used as reference values [33].

In terms of the modelling equations, the exponential formulations performed better than the other models tested (linear, logarithmic and square root), minimizing errors under higher fire risk scenarios (LFMC < 100%) both for the site-specific empirical models fitted in the study area (RMSE = 15%, MAE = 11%) and for the recalibration of previous models from another geographical area (RMSE = 16%, MAE = 12%). These findings regarding the exponential formulation are relevant and not previously reported in the literature. Previous studies involving empirical modelling of LFMC with remote sensing data primarily relied on linear regression analysis [22,33–35] or alternative nonlinear formulations [21]. Some authors also suggested more complex modelling approaches, such as artificial neural networks (ANNs) [36] or generalized additive models (GAMs) [21,23], with different results. In general terms, while the more complex models (e.g., GAMs) produced better fits during training and cross-validation, they were not well generalized in independent validation testing [21]. This is crucial for assessing model transferability and extrapolating predictions to new conditions beyond the calibration data [11].

Concerning the surface reflectance, the SI that included SWIR bands (NDII, NDWI and GVMI) were expected to provide much more direct estimates of LFMC, as they are directly related to plant water absorption [11,19]. Conversely, the SIs including visible and NIR (generally indicating vegetation greenness and growth) were better correlated in this

case, being indirectly linked with LFMC through the change in leaf pigment content [19,33]. Comparing the SI selected as inputs in the empirical models fitted in each geographical area (Madrid vs. Andalusia), we found that VARI yielded the highest correlation with LFMC in both cases. Marino et al. [21] reported the same result for this shrub species independently of the satellite sensor used (MODIS or Sentinel-2). Yebra et al. [26] also reported that VARI (in this case, derived from MODIS) was the SI that was most closely correlated with LFMC in *Cistus ladanifer* in a different Mediterranean site in Spain (the province of Toledo), located between the regions of Madrid and Andalusia. However, the best combination for predicting LFMC in Andalusia sites included VARI and EVI, whereas the best results in models fitted in the Madrid site were for the combination of VARI and SAVI. The different model inputs selected in both regions for the same shrubland species (EVI vs. SAVI) may explain some of the limitations for direct transfer of previous empirical models to other geographical areas. Our results highlight that, even for the same shrub species, some SI may be more affected by local site conditions than others (depending on the index formulation and the spectral bands included), providing differences in the spectral responses associated with the LFMC dynamics. EVI was originally developed from MODIS to enhance the sensitivity to a wider range of vegetation conditions, improving vegetation monitoring through decoupling of the canopy background signal and a reduction in atmospheric influences [37]. Previous studies also included EVI for LFMC estimation with different multispectral sensors, including Sentinel-2 [38] and MODIS [34,35]. Our findings suggest that the spectral variation due to different input sites can be addressed by simply recalibrating existing models. However, this approach requires sufficient field data for each new geographical area. Some authors suggest improving LFMC estimation with empirical models by using spectral data in a normalized form (i.e., difference between maximum and minimum SI values) [25,33]. This can better account for differences in cover, species composition and soil background between sites, especially for open shrublands [33]. The drawback of using the recalibration method proposed in the present study is that it requires a sufficient amount of in situ field data to correctly adapt the previous models to the environmental particularities of the new geographical site. Hence, once having invested in field monitoring in a certain region, fitting site-specific empirical models is preferred over recalibrating previous models from other regions, as it would enable more reliable LFMC prediction.

4.2. Temporal Transferability of LFMC Empirical Models for Wildfire Risk Assessment

The best empirical model fitted for *Cistus ladanifer* in the study area yielded a mean absolute error of 15% throughout the year in the independent validation dataset, decreasing to only 10% under the higher risk scenarios associated with lower LFMC values (<100%). This level of accuracy obtained with remote sensing data is considered very satisfactory for operational wildfire management, considering that LFMC values from destructive sampling in field monitoring provide a similar range of error (10–15%) [21]. Compared to previous LFMC studies with empirical modelling based on remote sensing, some authors have reported varying results in different types of Mediterranean shrubland [11,22,23]. Chuvieco et al. [11] assessed empirical models fitted in Cabañeros National Park (central Spain) in the years subsequent to the calibration period, reporting considerably lower accuracy compared to our models. However, these authors used empirical models that computed LFMC for a mixture of shrubland and grassland, reporting significantly different weather conditions than during the calibration period, which may have strongly affected the results, as herbaceous species exhibit a significantly faster and wider range of LFMC variability [21]. In the eastern Iberian Peninsula (Valencia region), Costa-Saura et al. [22] performed a short-term preliminary study also using empirical models with SI derived from Sentinal-2 as input variables. These authors reported similar prediction errors as in the present study but only assessed one summer season by cross-validation (June to October 2019). For the same study area (Valencia region), Arcos et al. [23] increased the LFMC field monitoring data (June 2020 to November 2021) and also reported good results

in independent validation for selected plots during the study period. However, to our knowledge, our study is the first attempt to assess the performance of empirical LFMC models derived from Sentinel-2 data in historical fire events occurring in previous years, i.e., validating temporal transferability outside data from years used in model calibration, which is crucial for operational wildfire risk assessment [11].

Our results regarding LFMC estimation with the best model, applied to historical wildfires occurring from 2018 to 2022 in the study area, indicated that the empirical model proposed based on spectral information from Sentinel-2 efficiently detected a decreasing trend in moisture content of *Cistus ladanifer* before wildfire occurrence. In all cases, LFMC values in this shrub species were below the threshold of 80% generally considered by the regional fire management service as indicating a high fire risk level in the early warning system, i.e., as a value associated with a significant increase in vegetation flammability [21]. Furthermore, larger wildfire events occurred when LFMC ranged from 60% to 70%. This is consistent with the threshold ascribed to other fire-prone Mediterranean-type shrubland (e.g., California chaparral), with critical LFMC values ranging from 60% to 80% [8,11,15,35,39]. Our study validates the performance of the empirical models for monitoring *Cistus ladanifer* as a fire-prone indicator species, suggesting a good potential for temporal transferability in predicting future wildfire events without further calibration. The proposed models will be further validated with new LFMC field data during the next wildfire seasons. Although more research is needed, the methods proposed in this study may also be useful in other shrubland with similar trends in LFMC dynamics and wildfire occurrence. Compared to similar studies assessing the performance of empirical models applied in different years, Arcos et al. [23] included not only SI derived from Sentinel-2 but also ancillary data, e.g., day of year (DOY) to account for seasonal variability of LFMC during the study period. However, this type of input variable may limit the effectiveness of temporal transferability of LFMC empirical models for operational fire risk assessment if they are not recalibrated with new field data, because wildfire occurrence throughout the year is being modified by climate change, with the fire season length being extended in the Mediterranean basin [5].

4.3. Future Research

This work demonstrates promising results for a very representative fire-prone species found in Mediterranean areas, providing empirical models that are useful for operational fire risk prediction based only on optical data from satellite remote sensing. However, future research should focus on LFMC modelling in other selected indicator species to cover a wider geographical range (e.g., *Cistus ladanifer* is less common in the eastern part of the region of Andalusia and other Mediterranean areas with calcareous soils). Field monitoring may be extended with additional plots to retrieve LFMC in other representative shrub species as reference values to explore the transferability of the proposed models and the identification of other potential indicator species for fire risk prediction in different ecosystem types [15]. For example, previous studies indicate that *Salvia rosmarinus* (i.e., *Rosmarinus officinalis* L.) and *Cistus albidus* may be good alternative indicator species for fire risk assessment in other Mediterranean locations due to the higher variability in moisture and more appropriate seasonal patterns than other widely distributed shrub species with less variable LFMC dynamics, such as *Quercus coccifera* [16,23,25,40].

Investing resources in field monitoring is also required to obtain sufficiently long time series for consistent empirical modelling [11,33], as well as to explore the proposed methods in tree species, grassland or mixed vegetation [12]. Other researchers have suggested use of the weighted average of LFMC accounting for each species' fractional cover in different types of vegetation [22,23,25,27], which may be useful when monospecific stands are not available regarding fire-prone indicator species. Predicting LFMC at a pixel level in wall-to-wall maps (i.e., independent of the species distribution) would be useful not only for fire risk monitoring but also for assessment of potential wildfire behaviour with simulation tools [41].

In addition to the vegetation type, LFMC variability is highly dependent on species phenology and weather conditions. Hence, empirical models based on spectral indices could be improved with the inclusion of ancillary variables, integrating spatial and temporal variability associated with climatic or geophysical characteristics [22,23,35], which may be useful for adding information indirectly related to vegetation status and development (e.g., physiology, weather, etc.). Historical seasonal trends are being modified and increasingly unpredictable due to climate change [5]. Caution should also be applied when considering the potential extrapolation of empirical models that rely on short time series of field data as reference values for calibration and validation, as LFMC estimation errors may be greatly increased when applied in new weather scenarios, even for the same site [11]. Therefore, topographic variables (i.e., slope, exposure, etc.) and weather inputs may be preferred to DOY-related variables to account for seasonal changes and interannual variability in improved empirical models combining spectral information from remote sensing and ancillary data.

5. Conclusions

The study findings confirm that empirical models derived from Sentinel-2 data provided accurate LFMC monitoring in fire-prone shrubland, with a mean absolute error (MAE) of 15% in the estimation of LFMC variability throughout the year and MAE decreasing to 10% for the critical lower LFMC values (<100%). The results also show that existing models could be easily recalibrated for extrapolation to a different geographical area with the same vegetation type, yielding similar errors to those of the empirical models specifically fitted in the study area in independent validation plots. However, while recalibration offers transferability, once investment has been made in field monitoring, site-specific models built with sufficient in situ data are likely to provide more reliable LFMC predictions. This research also demonstrates that the decrease in LFMC prior to historical wildfire events was accurately predicted by the empirical models. The findings confirmed the LFMC threshold of 80% as an adequate value for operational early warning systems based on this indicator shrub species, with LFMC values close to 60% being related to larger wildfire occurrence. For wildfire management at a regional level, initial investment in field monitoring during a limited period (e.g., 3–5 years) in selected vegetation (i.e., indicator species adapted to the particularities of the forest ecosystems) is strongly recommended for optimal monitoring of the spatial and temporal variability in LFMC and for predicting fire risk using empirical models based on remote sensing data.

Author Contributions: Conceptualization, E.M. and J.L.T.; methodology, E.M.; validation, E.M. and L.Y.; formal analysis, E.M.; investigation, E.M.; data curation, S.R., E.M., M.G. and J.M.; writing—original draft preparation, E.M.; writing—review and editing, L.Y., J.L.T. and J.M.; visualization, E.M.; supervision, E.M.; project administration, E.M., J.L.T., J.M. and F.S.; funding acquisition, E.M., J.L.T., J.M. and F.S. All authors have read and agreed to the published version of the manuscript.

Funding: This research was partially funded by Junta de Andalucía and EU Cross-Border Cooperation Programme INTERREG VA Spain-Portugal (POCTEP 2014-2020) within the frame of CILIFO project (Iberian Centre for Research and Forest Firefighting, 0753_CILIFO_5_E) and by the Spanish National Research Institute for Agriculture (INIA) through project VIS4FIRE (RTA2017-00042-C05-01) and co-funded by the EU-FEDER program.

Institutional Review Board Statement: Not applicable.

Informed Consent Statement: Not applicable.

Data Availability Statement: The datasets presented in this article are not readily available but could be shared upon reasonable request to the corresponding author.

Acknowledgments: The authors thank all the staff from INFOCA-Junta de Andalucía and ICIFOR-INIA forest fire research lab involved in field data gathering in the sampling plots during the study period.

Conflicts of Interest: E.M., L.Y. and J.L.T. are employed by Agresta company and received funding from Junta de Andalucía within the frame of CILIFO project (Iberian Centre for Research and Forest Firefighting). The rest of the authors declare no potential conflicts of interest.

Appendix A. Comparison of Empirical Models in Terms of Error Level in the Validation with LFMC Field Monitoring Data Available in the Region of Andalusia

Table A1. Prediction errors for validation (n = 335) after recalibration of empirical models previously fitted for the region of Madrid and extrapolated to LFMC sampling plots in the region of Andalusia (best values are indicated in bold).

Model	Formulation	All LFMC Range		LFMC < 100%	
		RMSE	MAE	RMSE	MAE
LR	LFMC = a + bVARI	22.01	17.65	19.75	15.71
MLR	LFMC = a + b·VARI + c·SAVI	22.21	17.18	18.43	13.69
NLR-log	LFMC = a + b·log(1 + VARI) + c·log(SAVI)	**21.91**	**17.07**	19.74	15.04
NLR-exp	LFMC = a·exp(b·VARI)·exp(c·SAVI)	23.52	18.25	**16.28**	**12.24**
NLR-sqr	LFMC = a + b·$(VARI)^{0.5}$ + c·$(SAVI)^{0.5}$	21.98	17.03	18.78	14.12

Table A2. Prediction errors for the independent validation (n = 111) of new empirical models fitted in LFMC sampling plots in the region of Andalusia (best values are indicated in bold). * MLR model fitted with logarithmic transformation of LFMC and spectral indices; ** MLR model fitted with logarithmic transformation of LFMC.

Model	Formulation	All LFMC Range		LFMC < 100%	
		RMSE	MAE	RMSE	MAE
MLR	LFMC = a + b·VARI + c·EVI	19.92	15.73	17.88	13.23
MLR-pot *	LFMC = a·$(1 + VARI)^{b}$·EVI^{c}	**19.75**	15.40	15.65	11.38
MLR-exp **	LFMC = a·exp(b·VARI)·exp(c· EVI)	19.78	**15.26**	**14.64**	**10.64**
NLR-log	LFMC = a + b·log(1 + VARI) + c·log(EVI)	20.25	16.10	19.61	14.80
NLR-exp	LFMC = a·exp(b·VARI)·exp(c· EVI)	19.89	15.53	15.67	11.53
NLR-sqr	LFMC = a + b·$(VARI)^{0.5}$ + c·$(EVI)^{0.5}$	19.86	15.71	18.85	14.04

Appendix B. Example of Extrapolation of an Empirical Model for LFMC Monitoring with Sentinel-2 Data in Historical Wildfire Events

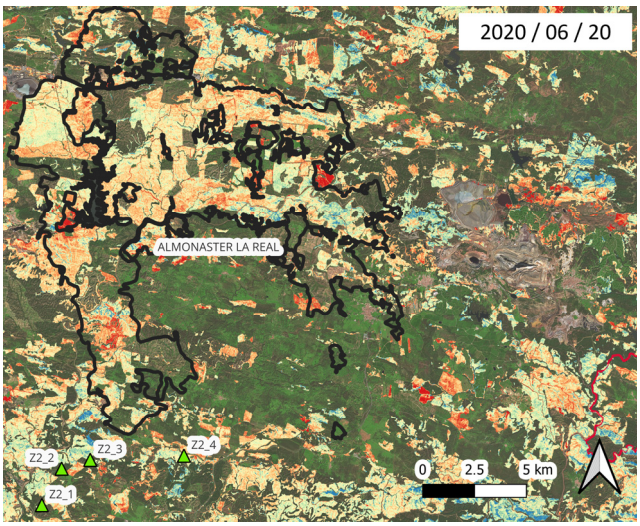

Figure A1. *Cont.*

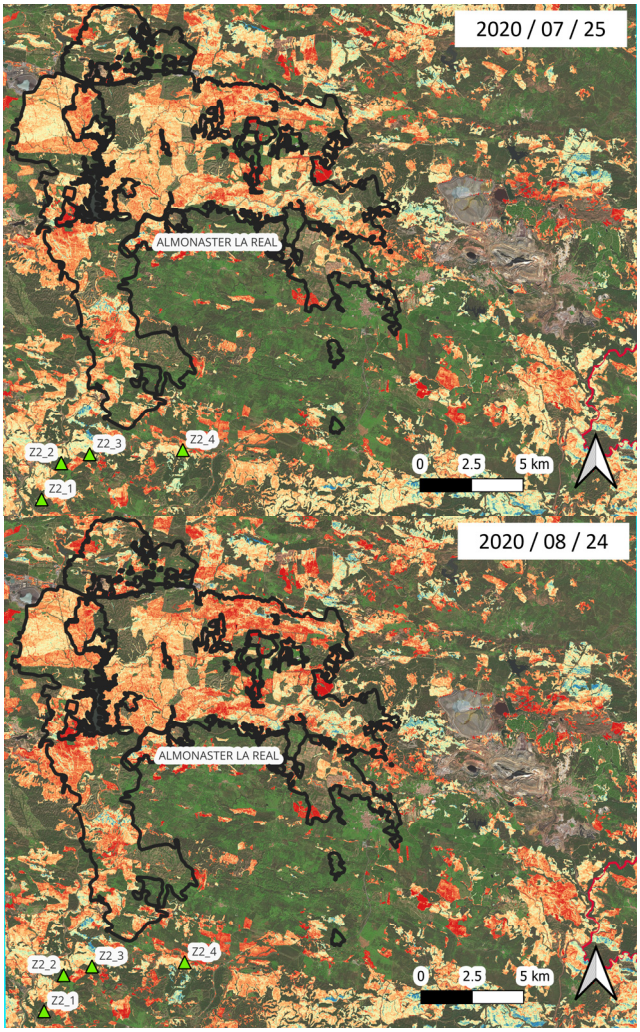

Figure A1. Changes in LFMC estimation obtained with the best empirical model derived from Sentinel-2 data in the Z2 pilot area before the Almonaster wildfire (ignited on 27 August 2020), which burned an area of 14,957 ha in 12 days (perimeter in black). This wildfire was the biggest event in the region of Andalusia during the study period (2018–2022). LFMC is only shown for pixels corresponding to shrubland. Reference plots used in Figure 7 for LFMC value calculations are depicted as green triangles.

References

1. Jolly, W.M.; Cochrane, M.A.; Freeborn, P.H.; Holden, Z.A.; Brown, T.J.; Williamson, G.J.; Bowman, D.M.J.S. Climate-induced variations in global wildfire danger from 1979 to 2013. *Nat. Commun.* **2015**, *6*, 7537. [CrossRef] [PubMed]
2. Boer, M.M.; Nolan, R.H.; De Dios, V.R.; Clarke, H.; Price, O.F.; Bradstock, R.A. ChangingWeather Extremes Call for Early Warning of Potential for Catastrophic Fire. *Earth's Futur.* **2017**, *5*, 1196–1202. [CrossRef]
3. Ruffault, J.; Curt, T.; Martin-StPaul, N.K.; Moron, V.; Trigo, R.M. Extreme wildfire events are linked to global-change-type droughts in the northern Mediterranean. *Nat. Hazards Earth Syst. Sci.* **2018**, *18*, 847–856. [CrossRef]
4. Turco, M.; Rosa-Cánovas, J.J.; Bedia, J.; Jerez, S.; Montávez, J.P.; Llasat, M.C.; Provenzale, A. Exacerbated fires in Mediterranean Europe due to anthropogenic warming projected with non-stationary climate-fire models. *Nat. Commun.* **2018**, *9*, 3821. [CrossRef] [PubMed]
5. Dupuy, J.-L.; Fargeon, H.; Martin-StPaul, N.; Pimont, P.; Ruffault, J.; Guijarro, M.; Hernando, C.; Madrigal, J.; Fernandes, P. Climate change impact on future wildfire danger and activity in Southern Europe: A Review. *Ann. For. Sci.* **2020**, *77*, 35. [CrossRef]
6. Jolly, W.M.; Johnson, D.M. Pyro-Ecophysiology: Shifting the Paradigm of Live Wildland Fuel Research. *Fire* **2018**, *1*, 8. [CrossRef]
7. Aguado, I.; Chuvieco, E.; Borén, R.; Nieto, H. Estimation of dead fuel moisture content from meteorological data in Mediterranean areas. Applications in fire danger assessment. *Int. J. Wildland Fire* **2007**, *16*, 390–393. [CrossRef]

8. Weise, D.R.; Zhou, X.; Sun, L.; Mahalingam, S. Fire spread in chaparral-'go or no go'? *Int. J. Wildland Fire* **2005**, *14*, 99–106. [CrossRef]
9. Marino, E.; Dupuy, J.L.; Pimont, F.; Guijarro, M.; Hernando, C.; Linn, R. Fuel bulk density and fuel moisture content effect on fire rate of spread: A comparison between FIRETEC model predictions and experimental results in shrub fuels. *J. Fire Sci.* **2012**, *30*, 277–299. [CrossRef]
10. Rossa, C.G.; Veloso, R.; Fernandes, P.M. A laboratory-based quantification of the effect of live fuel moisture content on fire spread rate. *Int. J. Wildland Fire* **2016**, *25*, 569–573. [CrossRef]
11. Chuvieco, E.; Aguado, I.; Cocero, D.; Riaño, D. Design of an empirical index to estimate fuel moisture content from NOAA-AVHRR images in forest fire danger studies. *Int. J. Remote Sensing* **2003**, *24*, 1621–1637. [CrossRef]
12. Luo, K.; Quan, X.; Binbin, H.; Yebra, M. Effects of Live Fuel Moisture Content on Wildfire Occurrence in Fire-Prone Regions over Southwest China. *Forests* **2019**, *10*, 887. [CrossRef]
13. Ruffault, J.; Martin-StPaul, N.; Pimont, F.; Dupuy, J.-L. How well do meteorological drought indices predict live fuel moisture content (LFMC)? An assessment for wildfire research and operations in Mediterranean ecosystems. *Agric. For. Meteorol.* **2018**, *262*, 391–401. [CrossRef]
14. Nolan, R.H.; Hedo, J.; Arteaga, C.; Sugai, T.; Resco de Dios, V. Physiological drought responses improve predictions of live fuel moisture dynamics in a Mediterranean forest. *Agric. For. Meteorol.* **2018**, *263*, 417–427. [CrossRef]
15. Pivovaroff, A.L.; Emery, N.; Sharifi, M.R.; Witter, M.; Keeley, J.E.; Rundel, P.W. The effect of ecophysiological traits on live fuel moisture content. *Fire* **2019**, *2*, 28. [CrossRef]
16. Ferrer, A.; Sánchez, P.; Borrego, C.; Jiménez, J.A.; Rodríguez y Silva, F. Estimation of moisture in live fuels in the mediterranean: Linear regressions and random forests. *J. Environ. Manag.* **2022**, *322*, 116069. [CrossRef] [PubMed]
17. Nolan, R.H.; Foster, B.; Griebel, A.; Choat, B.; Medlyn, B.E.; Yebra, M.; Younes, N.; Boer, M.M. Drought-related leaf functional traits control spatial and temporal dynamics of live fuel moisture content. *Agric. For. Meteorol.* **2022**, *319*, 108941. [CrossRef]
18. Peñuelas, J.; Rutishauser, T.; Filella, I. Phenology Feedbacks on Climate Change. *Science* **2009**, *324*, 887–888. [CrossRef]
19. Yebra, M.; Dennison, P.E.; Chuvieco, E.; Riaño, D.; Zylstra, P.; Hunt, E.R., Jr.; Danson, F.M.; Qi, Y.; Jurdao, S. A global review of remote sensing of live fuel moisture content for fire danger assessment: Moving towards operational products. *Remote Sens. Environ.* **2013**, *136*, 455–468. [CrossRef]
20. Chuvieco, E.; Aguado, I.; Salas, J.; García, M.; Yebra, M.; Oliva, P. Satellite Remote Sensing Contributions to Wildland Fire Science and Management. *Curr. For. Rep.* **2020**, *6*, 81–96. [CrossRef]
21. Marino, E.; Yebra, M.; Guillén-Climent, M.; Algeet, N.; Tomé, J.L.; Madrigal, J.; Guijarro, M.; Hernando, C. Investigating Live Fuel Moisture Content Estimation in Fire-Prone Shrubland from Remote Sensing Using Empirical Modelling and RTM Simulations. *Remote Sens.* **2020**, *12*, 2251. [CrossRef]
22. Costa-Saura, J.M.; Balaguer-Beser, Á.; Ruiz, L.A.; Pardo-Pascual, J.E.; Soriano-Sancho, J.L. Empirical Models for Spatio-Temporal Live Fuel Moisture Content Estimation in Mixed Mediterranean Vegetation Areas Using Sentinel-2 Indices and Meteorological Data. *Remote Sens.* **2021**, *13*, 3726. [CrossRef]
23. Arcos, M.A.; Edo-Botella, R.; Balaguer-Beser, Á.; Ruiz, L.Á. Analyzing Independent LFMC Empirical Models in the Mid-Mediterranean Region of Spain Attending to Vegetation Types and Bioclimatic Zones. *Forests* **2023**, *14*, 1299. [CrossRef]
24. Fan, L.; Wigneron, J.P.; Xiao, Q.; Al-Yaari, A.; Wen, J.; Martin-St Paul, N.; Dupuy, J.L.; Pimont, F.; Al Bitar, A.; Fernandez-Moran, R.; et al. Evaluation of microwave remote sensing for monitoring live fuel moisture content in the Mediterranean region. *Remote Sens. Environ.* **2018**, *205*, 210–223. [CrossRef]
25. Tanase, M.A.; Nova, J.P.G.; Marino, E.; Aponte, C.; Tomé, J.L.; Yáñez, L.; Madrigal, J.; Guijarro, M.; Hernando, C. Characterizing Live Fuel Moisture Content from Active and Passive Sensors in a Mediterranean Environment. *Forests* **2022**, *13*, 1846. [CrossRef]
26. Yebra, M.; Chuvieco, E.; Riaño, D. Estimation of live Fuel Moisture Content from MODIS images for fire risk assessment. *Agric. For. Meteorol.* **2008**, *148*, 523–536. [CrossRef]
27. Yebra, M.; Chuvieco, E. Linking ecological information and radiative transfer models to estimate fuel moisture content in the Mediterranean region of Spain: Solving the ill-posed inverse problem. *Remote Sens. Environ.* **2009**, *113*, 2403–2411. [CrossRef]
28. Jurdao, S.; Yebra, M.; Guerschman, J.P.; Chuvieco, E. Regional estimation of woodland moisture content by inverting Radiative Transfer Models. *Remote Sens. Environ.* **2013**, *132*, 59–70. [CrossRef]
29. Shu, Q.; Quan, X.; Yebra, M.; Liu, X.; Wang, L.; Zhang, Y. Evaluating the Sentinel-2A satellite data for fuel moisture content retrieval. In Proceedings of the IEEE International Geoscience and Remote Sensing Symposium, Yokohama, Japan, 28 July–2 August 2019; pp. 9416–9419.
30. Hernández-Rodríguez, M.; Martín-Pinto, P.; Oria-de-Rueda, J.A.; Diaz-Balteiro, L. Optimal management of Cistus ladanifer shrublands for biomass and Boletus edulis mushroom production. *Agrofor. Syst.* **2017**, *91*, 663–676. [CrossRef]
31. Montero, G.; López-Leiva, C.; Ruiz-Peinado, R.; López-Senespleda, E.; Onrubia, R.; Pasalodos, M. *Producción de Biomasa y Fijación de Carbono por los Matorrales Españoles y por el Horizonte Orgánico Superficieal de los Suelos Forestales*; Ministerio de Agricultura, Pesca y Alimentación: Madrid, Spain, 2020; 225p.
32. R Core Team. R: The R Project for Statistical Computing. Available online: https://www.r-project.org/ (accessed on 13 May 2024).
33. Lai, G.; Quan, X.; Yebra, M.; He, B. Model-driven estimation of closed and open shrublands live fuel moisture content. *GIScience Remote Sens.* **2022**, *59*, 1837–1856. [CrossRef]

34. Arganaraz, J.P.; Landi, M.A.; Bravo, S.J.; Gavier-Pizarro, G.I.; Scavuzzo, C.M.; Bellis, L.M. Estimation of Live Fuel Moisture Content from MODIS Images for Fire Danger Assessment in Southern Gran Chaco. *IEEE J. Sel. Top. Appl. Earth Obs. Remote Sens.* **2016**, *9*, 5339–5349. [CrossRef]
35. Myoung, B.; Kim, S.H.; Nghiem, S.V.; Jia, S.; Whitney, K.; Kafatos, M.C. Estimating Live Fuel Moisture from MODIS Satellite Data for Wildfire Danger Assessment in Southern California USA. *Remote Sens.* **2018**, *10*, 87. [CrossRef]
36. Adab, H.; Kanniah, K.D.; Beringer, J. Estimating and up-scaling fuel moisture and leaf dry matter content of a temperate humid forest using multi resolution remote sensing data. *Remote Sens.* **2016**, *8*, 961. [CrossRef]
37. Huete, A.; Didan, K.; Miura, T.; Rodriguez, E.P.; Gao, X.; Ferreira, L.G. Overview of the radiometric and biophysical performance of the MODIS vegetation indices. *Remote Sens. Environ.* **2002**, *83*, 195–213. [CrossRef]
38. Marino, E.; Guillén-Climent, M.; Algeet, N.; Tomé, J.L.; Hernando, C. Estimation of live fuel moisture content of shrubland using MODIS and Sentinel-2 images. In *Advances in Forest Fire Research 2018*; Chapter 2—Fuel Management; Viegas, D.X., Ed.; Imprensa da Universidade de Coimbra: Coimbra, Portugal, 2018; pp. 218–226.
39. Dennison, P.E.; Roberts, D.A.; Peterson, S.H.; Rechel, J. Use of Normalized Difference Water Index for monitoring live fuel moisture. *Int. J. Remote Sens.* **2005**, *26*, 1035–1042. [CrossRef]
40. Martin-StPaul, N.; Pimont, F.; Dupuy, J.L.; Rigolot, E.; Ruffault, J.; Fargeon, H.; Cabane, E.; Duché, Y.; Savazzi, R.; Toutchkov, M. Live Fuel Moisture Content (LFMC) Time Series for Multiple Sites and Species in the French Mediterranean Area since 1996. *Ann. For. Sci.* **2018**, *75*, 57. [CrossRef]
41. Salis, M.; Del Giudice, L.; Jahdi, R.; Alcasena-Urdiroz, F.; Scarpa, C.; Pellizzaro, G.; Bacciu, V.; Schirru, M.; Ventura, A.; Casula, M.; et al. Spatial Patterns and Intensity of Land Abandonment Drive Wildfire Hazard and Likelihood in Mediterranean Agropastoral Areas. *Land* **2022**, *11*, 1942. [CrossRef]

Disclaimer/Publisher's Note: The statements, opinions and data contained in all publications are solely those of the individual author(s) and contributor(s) and not of MDPI and/or the editor(s). MDPI and/or the editor(s) disclaim responsibility for any injury to people or property resulting from any ideas, methods, instructions or products referred to in the content.